LA-UR-81-623

CONF-810507--1

TITLE: DYNAMIC MATERIAL PROPERTY MEASUREMENTS USING AN IMPROVEMENT OF THE FREELY EXPANDING RING TECHNIQUE

AUTHOR(S): T. A. Duffey, M-4 Visiting Staff Member
R. R. Karpp, M-4
R. H. Warnes, M-4
J. D. Jacobson, M-4
A. E. Carden, Visiting Staff Member

MASTER

SUBMITTED TO: Society for Experimental Stress Analysis
Speakers, 1981 SESA Spring Meeting
Dearborn, Michigan
May 31 - June 5, 1981

University of California

LOS ALAMOS SCIENTIFIC LABORATORY
Post Office Box 1663 Los Alamos, New Mexico 87545
An Affirmative Action/Equal Opportunity Employer

Form No. 836 R3
St. No. 2629
12/78

UNITED STATES
DEPARTMENT OF ENERGY
CONTRACT W-7405-ENG. 36

DYNAMIC MATERIAL PROPERTY MEASUREMENTS USING AN IMPROVEMENT OF THE FREELY EXPANDING RING TECHNIQUE

T. A. Duffey*
R. R. Karpp
R. H. Warnes
J. D. Jacobson
A. E. Carden**

Group M-4, MS-940
Los Alamos National Laboratory
Los Alamos, New Mexico 87545

ABSTRACT

Improvements to the expanding ring test for determination of dynamic material properties are described. The improvements alleviate previous difficulties associated with double-differentiation of ring displacement-time data. The technique is illustrated utilizing 6061-0 and 6061-T6 aluminum rings expanded well into the plastic range at strain rates up to 10^4/s. Two-dimensional numerical investigations of the expansion process qualitatively predict observed results and clarify the range over which data is useful for determining material properties.

INTRODUCTION

Since its introduction nearly two decades ago, the expanding ring test has shown considerable promise as a simple method of obtaining strain-rate-sensitive uniaxial stress property data. The procedure is to monitor the radial motion of a freely expanding ring. The stress-strain-strain rate response of the ring material can then be calculated from the ring equation of motion and the recorded data.

The authors have recently presented preliminary results[1] on a modification to the expanding ring test that overcomes the double differentiation difficulty encountered by others using displacement-time expanding ring data to calculate stress.[2,3] The procedure used is to directly measure the radial velocity-time of the uniformly expanding ring by means of a laser velocity interferometer.[4] By both integrating and differentiating the velocity-time data only once, dynamic stress-strain curves for a material at various values of strain rate are deduced and presented in the form of three-dimensional stress-strain- strain rate curves.

It is the purpose of the present peper to describe improvements and applications of the method reported in Ref. 1. Expanding ring experimental results on 6061-0 and 6061-T6 aluminum are described over a wide range of strain rates. These experimental results are used to illustrate improvements in the previous data reduction techniques. In addition, the experimental results are compared with two-dimensional numerical calculations that were performed to increase the understanding of the detailed phenomenology of the expanding ring. These calculations, which include the effects of wave propagation through the ring as well as axial material motions, were performed with a hydrodynamic computer program.

GOVERNING RING EQUATIONS

The circumferential stress, σ, in a thin ring of radius r undergoing symmetrical radial motion, derived from Newton's Second Law, is

$$\sigma = -\rho r \ddot{r} \quad . \tag{1}$$

---

* Permanent address: Department of Mechanical Engineering, University of New Mexico, Albuquerque, New Mexico 87131
** Permanent address: AME Department, University of Alabama, University, Alabama 35486

where ρ is mass density of the ring material and $\ddot{r}$ is radial acceleration. If one assumes that plastic strains conserve volume and the elastic volume change is negligible, then density does not change with ring expansion and Eq. (1) can be shown to be based on current cross-sectional area; i.e., σ represents true stress.

True strain is given by $\varepsilon = \ln(r/r_o)$ where r_o = initial ring radius. True strain rate then becomes $\dot{\varepsilon} = \dot{r}/r$.

Determination of dynamic stress-strain-strain rate contours is conceptually quite simple. The ring initially undergoes a rapid acceleration; then, as the ring expands outward, its radial velocity, $\dot{r}$, decreases because of the opposing hoop stress, σ. Based only upon radial ring velocity $\dot{r}(t)$, as measured directly by the velocity interferometer at some time t, it is possible to calculate radial displacement, $r(t)$, by numerical integration and radial acceleration, $\ddot{r}(t)$, by a single numerical differentiation. The stress-strain-strain rate point at that instant of time, t, can then be determined by appropriate application of the above equations.

In this work we assume that the stress-strain-strain rate behavior can be represented by a surface in three-space, and, for purposes of illustration of the expanding ring technique, results are presented in stress-strain-strain rate space. The trajectory of a given expanding ring is represented by a single curved line in stress-strain-strain rate space with strain rate monotonically decreasing and strain monotonically increasing when the material is deforming plastically. By running several experiments for a given material over a range of initial strain rates, a series of lines is plotted in this three-space and a surface will emerge. Quasi-static data, which should also fall on this surface, can then be plotted on the $\dot{\varepsilon} = 0$ plane for comparison if desired.

EXPERIMENTAL PROGRAM

Ring-Driver System

The experiment is constructed as shown in Fig. 1. A ring of the material to be studied is press-fitted onto a steel cylindrical driver. The press-fit insures good contact between the ring and driver and pre-loads the ring to a hoop stress about equal to the yield strength. Subsequent radial displacement is essentially all plastic. A cylinder of high explosive is centered inside the driver and detonators are placed on both ends of the explosive. A field lens is placed approximately a focal length from the surface of the ring and the beam from a laser is focussed to a small spot on the ring that has been slightly roughened to diffusely reflect the beam. The lens also acts as a collector for this reflected beam, sending it back to the interferometer as a broad, parallel beam. The steel driver and ring are designed so that when the explosive detonates, the driver undergoes elastic and slightly plastic expansion. The thin ring, however, separates from the driver and undergoes large plastic deformations as its initial kinetic energy is dissipated into plastic work.

Velocity Interferometer System

Figure 2 shows a simplified schematic of the interferometer system. The return beam is reduced in size, split, and directed into two interferometers, the sensitivities of which can be adjusted independently. The interferometer layout is similar to the VISAR developed by Barker and Hollenbach.[4] Because we needed greater velocity sensitivity than is normally possible with the VISAR using etalons as optical delays, a modified version of an air delay leg suggested by Amery[5] was incorporated into the high sensitivity interferometer on these experiments. Details of the interferometer and the data reduction are in Refs. 4 and 5. Briefly, the frequency of the return beam reflected from the moving target is Doppler-shifted by an amount proportional to the velocity of the target. In the individual interferometers, the beam is split and the light traversing one leg of the interferometer is delayed a small amount relative to the other leg (typically a few tenths of a nanosecond to as much as 20 nanoseconds). Thus, the two beams that are combined to give interference were reflected from the target at two different times. If the target is accelerating, these two beams will have slightly different frequencies and the resulting difference frequency is detected by photomultipliers and recorded on oscilloscopes. These traces provide a continuous record of the target velocity to within a few meters/second.

Experiments Conducted

Materials on which expanding ring experiments have been conducted to date include hardened and annealed copper, 6061-T6 and 6061-O aluminum, lead, uranium-6% niobium alloy, as well as rocket propellant. The parameters varied in these tests are the mass of explosive and the size of the driver/ring system. Numerous identical experiments have been performed to check on reproducibility of the data.

THEORETICAL INVESTIGATION OF TWO-DIMENSIONAL EFFECTS

A typical velocity-time curve from an expanding ring test with annealed aluminum is shown in Fig. 3. Four regions, each having a somewhat different behavior, can be identified. Region I contains the initial ring acceleration caused by the shock wave reflection at the ring surface and also includes the subsequent radial wave reflections. Region II starts after the radial wave motion has damped and contains a period of rapidly decreasing velocity with the deceleration higher in the beginning and lower near the end of the region. Region III contains a period of fairly constant deceleration. The arrival of the first unwanted disturbance marks the beginning of Region IV. Velocity-time data from Regions I or IV obviously cannot be used to infer stress. The

primary data window is Region III, and a central question concerning the interpretation of the data is whether or not data from Region II should be used to infer flow stress of the test material.

To investigate details of the driver-ring interaction, several two-dimensional, finite-difference calculations were made. These calculations were performed with a Lagrangian continuum mechanics code similar to the one described by Wilkins.[6] To simplify the calculation, the driver was initially given a uniform outward radial velocity, and the test ring was initially motionless. Although this configuration is highly simplified compared to the motion induced by the detonation of an explosive, it is assumed to contain the essence of the launch process.

Figure 4a shows a calculated velocity-time curve for an aluminum ring with a yield strength in tension of 0.18 GPa. The initial radial velocity of the driver was 100 m/s, and the velocity plotted in Fig. 4a is for the point on the ring which is observed by the interferometer. For this calculation, the material was treated as elastic-perfectly plastic. Regions I, II, and III can clearly be identified in the calculated velocity-time curve of Fig. 4a. Figure 4b shows the velocity-time curve for a calculation that is nearly identical to the one that produced Fig. 4a, but this calculation was for a one-dimensional problem; i.e., both driver and ring were assumed to be long cylinders. Region II does not appear in the one-dimensional velocity-time curve of Fig. 4b. From these calculated results, one concludes that Region II, the period of rapidly decreasing velocity and deceleration, can result from two-dimensional flow effects in materials that are not rate sensitive. Therefore, in the expanding ring test, care must be taken to avoid the use of data that may be affected by two-dimensional effects.

Data Reduction Technique and Results

The final analysis of these experiments requires smoothing and subsequent differentiation and integration of the numerical data $f(t)$. Spline functions are often recommended for this purpose because their extreme flexibility and strong local properties make them unlikely to introduce the bias often exhibited by more rigid models such as global polynomials.[7] The spline function proposed by Reinsch[8,9] is used here. The method contains a parameter that serves as a convenient smoothing control. The method is illustrated in Fig. 5. The effect of smoothing $f(t)$ with the Reinsch algorithm for three variations in the smoothing parameter can be seen. Evaluation of the smoothing function and its derivative and integral results in values of smoothed radial displacement, velocity, and acceleration that together with the ring equations given earlier, determine stress-strain-strain rate triples.

Figure 6 is a stress-strain curve (including elastic unloading) obtained with what appeared to be optimal smoothing. A summary of the data obtained in this way is displayed in stress-strain-strain rate space for 6061-T6 aluminum and 6061-O aluminum in Figs. 7 and 8, respectively. The beginnings of a stress-strain-strain rate surface are seen to emerge, with stress levels (at a given strain) generally increasing slightly with rate of strain.

CONCLUSIONS

Methods have been presented herein for improving the well-known expanding ring experiment for dynamic material property determinations. The new procedure, which incorporates a velocity interferometer for direct ring velocity-time measurements, overcomes previous difficulties associated with double differentiation of ring displacement-time data.

An improved scheme for data reduction and development of stress-strain-strain rate surfaces are described. Finally, results of a detailed, two dimensional analysis of the ring expansion process are presented and compared with experimentally recorded velocity-time data. Experimental and calculational velocity-time traces are in good agreement, and the comparisons serve to delineate the useful range over which the ring data provide reliable material property information.

ACKNOWLEDGMENTS

The authors gratefully acknowledge the contributions of Thomas E. Gould and Gilbert L. Sanchez for preparation of the experiments, and of Elaine F. Alei for reduction of the data.

REFERENCES

1. R. H. Warnes, et al, "An Improved Technique for Determining Dynamic Material Properties Using the Expanding Ring," presented at Int. Conf. Metallurgical Effects on High Strain-Rate Deformation and Fabrication, Albuquerque, N.M., June 22-26, 1980.

2. P. C. Johnson, et al, "Measurement of Dynamic Plastic Flow Properties Under Uniform Stress," Symposium on the Dynamic Behavior of Materials, ASTM Special Publication No. 336, p. 195 (1963).

3. C. R. Hoggatt and R. F. Recht, Exp. Mech., 9, p. 441 (1969).

4. L. M. Barker and R. E. Hollenbach, J. Appl. Phys., 43, p. 4669 (1972).

5. B. T. Amery, Proceedings of the Sixth Symposium (International) on Detonation, D. J. Edwards (ed.), Office of Naval Research, Department of the Navy, ACR-221, p. 673 (1976).

6. M. L. Wilkins, Calculation of Elastic-Plastic Flow, University of California, Lawrence Radiation Laboratory report, UCRL-7322, Rev. I (January 8, 1970).

7. S. Wold, Technometrics, 16, p. 1 (1974).

8. C. H. Reinsch, Numerische Mathematik, 10, p. 177 (1967).

9. C. H. Reinsch, Numerische Mathmeatik, 16, p. 451 (1971).

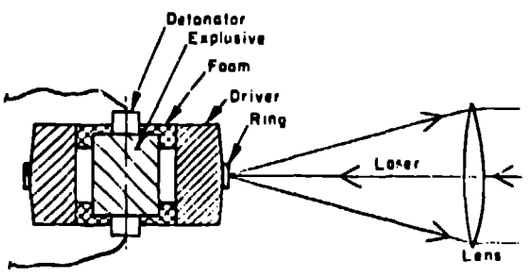

Fig. 1
Cross-Sectional View of the Experiment

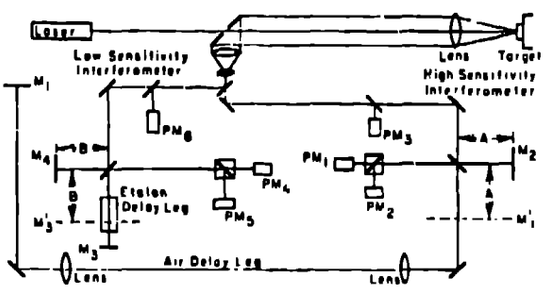

Fig. 2
Simplified schematic of the laser velocity interferometer system used on these experiments. Each of the two separate interferometers has a photomultiplier (PM), monitoring the return light and two PM's recording the interference information. Additional optics (not shown) permit quadrature recording of the interference information, enabling the sign of the target acceleration to be determined.

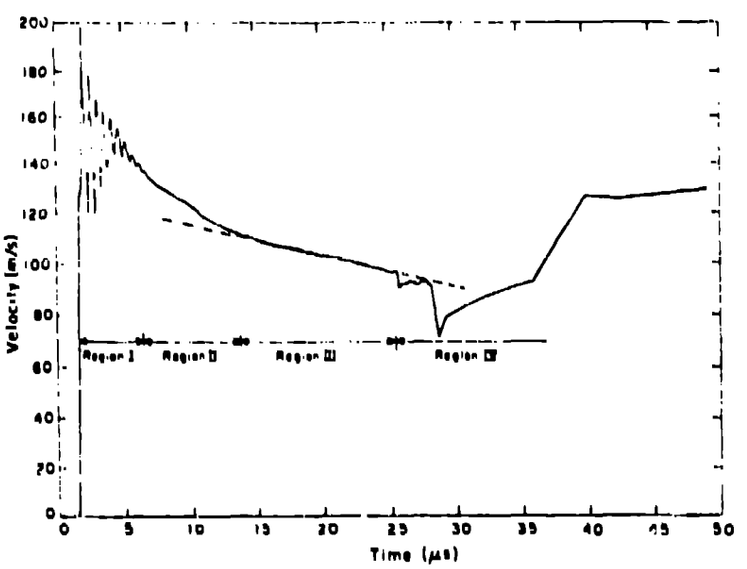

Fig. 3
Typical Velocity-Time Curve for 6061-O Aluminum

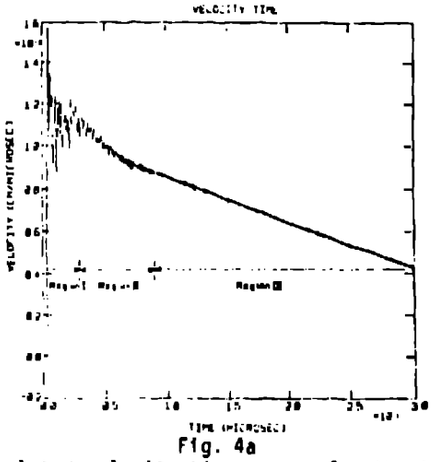

Fig. 4a

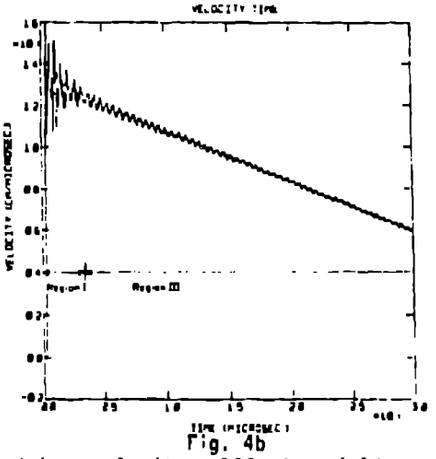

Fig. 4b

Calculated velocity-time curves for the test ring. Fig. 4a. driver velocity 100 m/s, yield strength = 0.18 GPa. Fig. 4b: calculation with motion restricted to the radial direction only. Driver velocity = 100 m/s, yield strength = 0.18 GPa.

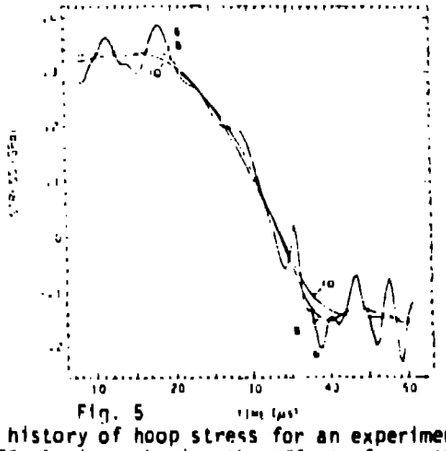

Fig. 5

The history of hoop stress for an experiment on 6061-T6 aluminum showing the effect of smoothing $\dot{r}(t)$ with the Reinsch algorithm. The parameter is assigned standard deviation in cm/s.

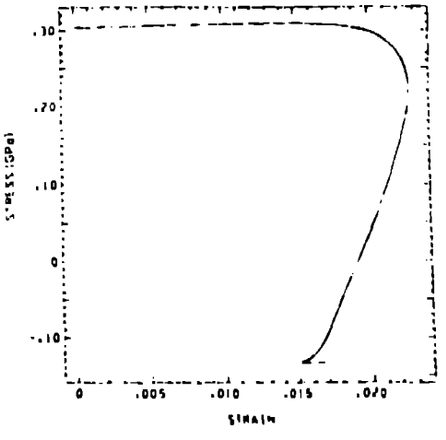

Fig. 6

The response of 6061-T6 aluminum determined from the data of Fig. 5

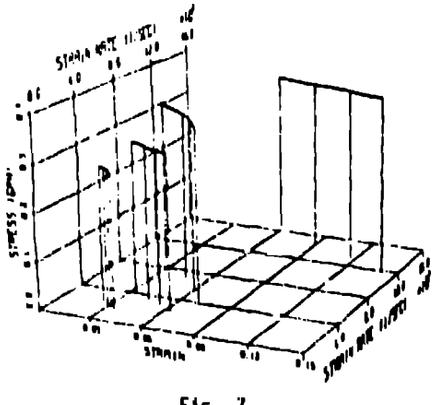

Fig. 7

Stress-strain-strain rate plot of data from expanding ring tests on 6061-T6 aluminum.

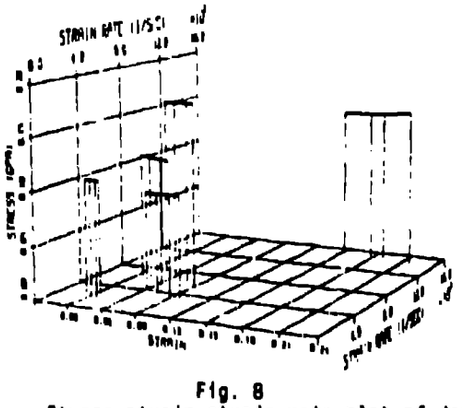

Fig. 8

Stress-strain strain rate plot of data from expanding ring tests on 6061-0 aluminum.